ORNI/Sub/94-SS110/04

DEVELOPMENT OF CVD MULLITE COATINGS FOR SiC FIBERS

March 15, 2000

Report Prepared by
Vinod K. Sarin and Sesha Varadarajan
Boston University
15, St. Mary's Street
Boston, MA-02134

under
ORNL/Sub/94-SS110/04

for

OAK RIDGE NATIONAL LABORATORY
Oak Ridge, TN 37831
Managed by

LOACKEED MARTIN ENERGY RESEARCH CORP.
for the
U.S. Department of Energy
under contract DE-AC05-96OR22464

DISCLAIMER

ORNl/Sub/94-SS110/04

DEVELOPMENT OF CVD MULLITE COATINGS FOR SiC FIBERS

March 15, 2000

Research sponsored by the U.S.Department of Energy,
Office of Fossil Energy
Advanced Research and Technology Development Material Program

Report Prepared by
Vinod K. Sarin and Sesha Varadarajan
Boston University
15, St. Mary's Street
Boston, MA-02134

under
ORNL/Sub/94-SS110/04

for

OAK RIDGE NATIONAL LABORATORY
Oak Ridge, TN 37831
Managed by

LOACKEED MARTIN ENERGY RESEARCH CORP.
for the
U.S. Department of Energy
under contract DE-AC05-96OR22464

CONTENTS

ABSTRACT

A process for depositing CVD mullite coatings on SiC fibers for enhanced oxidation and corrosion, and/or act as an interfacial protective barrier has been developed. Process optimization via systematic investigation of system parameters yielded uniform crystalline mullite coatings on SiC fibers. Structural characterization has allowed for tailoring of coating structure and therefore properties. High temperature oxidation/corrosion testing of the optimized coatings has shown that the coatings remain adherent and protective for extended periods. However, preliminary tests of coated fibers showed considerable degradation in tensile strength.

Research sponsored by the U.S. Department of Energy, Fossil Energy Advanced Research and Technology Development Materials Program, DOE/FE AA 15 10 10 0, Work breakdown structure element BU-2.

1.0 INTRODUCTION

Increased operating temperatures to achieve higher efficiencies in several industrial applications have generated the need for new structural materials for components such as hot gas filters, heat exchangers, and gas turbine combustion liners. Ceramic matrix composites like SiC_f/SiC owing to their oxidation resistance and mechanical properties at elevated temperature have been identified as a leading candidate material for many such applications [1]. Currently the use of these composites is being limited due to fiber degradation at the fiber-matrix interface either during processing or subsequent high temperature service. In monolithic SiC, the formation of a thin silica layer at moderate temperatures has been shown to reduce the rate of further oxidation [2]. However, the non-stoichiometric nature of commercially available SiC fibers modifies the rate of oxygen diffusion through the scale resulting in active oxidation and corrosion [3]. Thus the development of an interfacial coating to protect SiC fibers is critical for the utilization of ceramic composites for such applications. This presents a major technical challenge since the interlayer must be thermodynamically compatible with the fiber and matrix, control stresses and frictional forces within the composite, and be environmentally stable.

Carbon whether deposited on the fibers prior to consolidation [4] or formed during processing [5] is the most commonly used interlayer in ceramic composites. A highly oriented graphite layer has been found to perform well in Nicalon fiber reinforced SiC matrix composites, yielding exceptional mechanical properties via reduction in interfacial

stresses [1]. However, the poor oxidation resistance of carbon over 400°C results in fiber degradation via attack of the carbon coating at the exposed fiber ends [6].

Several alternative coatings to overcome the deficiencies of carbon have been investigated. So far hexagonal BN coatings have shown the most promise. This is not surprising since mechanically BN behaves like carbon [6], but has significantly better oxidation resistance. However, the presence of inherent oxygen in these coatings decomposes the fibers leading to both loss of strength and oxidation resistance. Other potential coatings like TaC, ZrC also suffer from similar oxygen contamination problems [7].

Mullite ($3Al_2O_3 \bullet 2SiO_2$), due to its unique properties such as thermal expansion match with SiC, oxidation resistance, elevated temperatures mechanical and compositional stability has been targeted as a candidate material [8-10]. However, attempts to deposit mullite coatings by various processing conditions have met with limited success [11]. Several of the techniques developed require a high temperature post-heat treatment to convert amorphous alumina-silica into crystalline mullite, which results in fiber decomposition and micro-porosity [12-13]. Plasma spray deposition of mullite as a corrosion barrier coating has been reported [14], but since the resultant coatings are thick, non-uniform, and contain pores, they are unsuitable as a interfacial coating. Additionally, grit blasting is used to enhance adherence which not only degrades strength but is unusable for fiber tows. To overcome these problems, a process to chemically vapor deposited mullite coatings has been developed and patented at

Boston University [15]. In the present investigation this process is being modified to develop an oxidation resistant interfacial barrier coating for SiC fibers.

2.0 EXPERIMENTAL DETAILS

2.1 CVD Process

Commercially available, organo-metallic precursor derived SiC fibers, namely Nicalon, Hi-Nicalon and Tyranno were used as substrates. The organic sizing on the as-received fiber tows was removed by heating them in air at 375°C for 4 hours. A vertical hot walled reactor CVD unit was used to deposit the coatings. The fibers were gripped in clips and inserted into a 95 mm long coating tube (Fig.1). The diameter of the coating tube could be varied to get different gas flow velocities. An axial temperature gradient of about 8° was maintained to partially overcome axial depletion. The effect of process parameters such as input gas velocity, system pressure, and partial pressure of metallic chlorides (P_{MClx}) was investigated at a fixed substrate temperature of 972 ± 4°. The coated fibers were characterized using SEM and XRD.

2.2 Oxidation Testing

Oxidation tests were carried out in oxygen between 1000°C to 1300°C for 100 to 200 h. The flow rate of oxygen was varied from 500 ccm to 1000 ccm. Weight measurements were taken every 25 hours by interrupting the experiment. Since oxygen flow was maintained while the furnace ramped down at 4°C/min, the actual duration of the test was actually slightly longer then reported. The uncoated samples used in these tests were "desized" and subsequently heated in the CVD reactor to mimic coating

conditions. This ensured that the oxidation results were not influenced by weight loss due to "desizing" or volatilization.

2.3 Cyclic Oxidation Testing

Cyclic oxidation testing was performed at 1000°C in a reciprocating furnace with a 1-hour heating and 1-hour cooling cycle. An oxygen flow of 250 ccm was maintained throughout the cycle. Samples reached the set temperature in about 10 minutes, while forced cooling with a fan resulted in the fibers cooling to ~50°C in about 25 minutes. Weight measurements were made after 10, 100 and 250 cycles.

2.4 Corrosion Testing

Coated and un-coated fibers were loaded with approximately 0.15 mg/cm^2 of Na_2SO_4. Hot corrosion tests were performed on these fibers at 1100°C in a horizontal tube furnace and at an oxygen flow rate of 250 ccm. Weight measurements were made every 25 hours by interrupting the experiment. Entire fiber tows were used to facilitate handling for taking weight measurements. However, this created some problems, as it was not possible to coat all the fibers of the tow uniformly.

2.5 Tensile Testing

Dr. Edgar Lara Curzio of Oak Ridge National Laboratory performed some very preliminary single fiber tensile test on mullite coated SiC fibers. Individual fibers were picked up using cellophane tape and mounted on cardboard holders with epoxy. The cardboard was cut along the center, so as to transfer the applied load to the fiber, and

pulled in tension. To account for variations in fiber diameter, an average of 25 fibers from each tow were tested.

3.0 RESULTS AND DISCUSSION

Initial CVD coating experiments yielded tows having several undesirable characteristics such as brittleness, bridging in fibers, and non-uniform coatings. For example, initial bridging of the fibers (Fig.2) resulted in brittleness of the tows and also prevented the inside of the tows from being coated. This phenomena was by radial depletion of the reactants as they flowed from the outside to the inside of the tow diameter. It was determined that by increasing gas flow velocity and thus reducing growth rate, bridging could be reduced or eliminated. Experimental results showed that at gas flow velocities above 600 cm/s bridging was completely eliminated. Additionally it was observed that by increasing the gas flow velocities further into the 600-800 cm/s regime, the problem of axial depletion was also alleviated and ~85 mm long fiber tows could be uniformly coated.

Surface morphology and the cross-section of a typical mullite coating on Nicalon fibers is shown in Fig.3. The coatings were observed to be dense, uniform in thickness (about 1μ) with a fine-grained equiaxed structure. X-ray diffraction studies confirmed that the only crystalline phase present was mullite (Fig.4). X-ray analysis of mullite coatings on fibers usually showed distinct {(ab0) (ba0)} type peaks, indicating a normal orthorhombic structure. However, coatings grown on monolithic SiC substrates were observed to be typically tetragonal in structure [16]. The difference is probably due to

combination of factors. Firstly, compositional since the Al/Si ratio measured on the surface of the coated fibers was found to be lower than that measured on coatings on monolithic SiC. As has been previously reported [17], mullite coatings have been found to show an increase in their Al_2O_3 content, which drives the structure to become tetragonal, with an increase in coating thickness. Since the fibers had significantly thinner coatings, this compositional/structural difference can in a way be attributed to coating thickness. Secondly, it has been established that the tetragonal structure formed on monolithic SiC is not stable. Thus, the orthorhombic structures formed on the fibers may in part be due to the lower growth rates (0.66μm/hr vs. 5μm/hr) used for fibers, giving more time for equilibrium (stable) structure to be formed during growth of the coating.

3.1 Effect of System Parameters

3.1.1 System pressure

The system pressure was varied from 25 torr to 122 torr keeping all other parameters constant. Tubes of different diameters were used to introduce the gas and maintain the same gas flow velocity over the substrate regardless of the system pressure. This resulted in a fixed residence time assuming that the gas velocity changed with a change in the tube cross-section. To minimize possible errors due to this assumption all coating thickness measurements (growth rate) were done at the midpoint of the sample. Achieving fixed residence time by varying the amounts of dilutant gas, was not investigated due to:

i) Possible shift of the optimum deposition zone, higher or lower depending on whether the velocity increased or decreased.

ii) Different viscosity's of the dilutant gas when compared to the reactant mixture giving rise to different boundary layer profiles.

Growth rate was found to increase at an exponential rate with increasing pressure (Fig.5). A similar study performed on monolithic SiC substrates showed linear increase in growth rate followed by a decrease in growth rate due to depletion [18]. The difference in trends is probably due to the higher gas velocity used for deposition on the fiber tows, which effectively reduces depletion. The surface morphology of the coating obtained on fibers are shown in Fig.5. At 25 and 50 torr very fine nano-crystalline grains (50-100 nm) were observed on the surface. At 80 torr, the coatings had relatively equiaxed grains and were uniform in thickness. However at 125 torr, the coatings had varied surface morphology along the diameter of the tows and were non-uniform.

3.1.2 Input gas velocity

The linear gas flow velocity or rather the residence time of the gaseous species in the hot zone of the reactor was found to strongly influence homogenous gas phase nucleation and growth rate. Mullite coatings were grown for 75 minutes using different gas flow velocities while keeping all other parameters constant (Fig.6). It can be seen that growth rate has an even stronger exponential dependence on velocity than system pressure. The surface morphology showed a trend towards larger grain sizes with decrease in gas flow velocity, because of a lack of the effect of gas depletion. However,

if the same tests were to be performed at a much lower average velocity, it is projected that the growth rate may not show such a strong dependence on the velocity, mainly due to depletion effects.

3.1.3 Al/Si molar ratios

The Al/Si molar ratio of the input gas was experimentally varied by i) holding the Al/Si ratio constant while changing the total partial pressure of metallic chlorides, and ii) holding the total partial pressure of metallic chlorides constant while changing the Al/Si ratio.

The effect of partial pressure of metallic chlorides (sum of the partial pressures of $AlCl_3$ and $SiCl_4$) on coating thickness for a fixed Al/Si ratio of 3:1 was investigated in the 0.25 to 0.70 torr range (Fig.7). Typical fine-grained microstructures were observed in all the samples, while X-ray diffraction indicated no differences in crystallanity. The observed decrease in growth rate at partial pressures greater than 0.53 torr is probably due to increased gas phase nucleation and depletion.

The effect of varying Al/Si ratios on growth rate, while keeping the partial pressure of metallic chlorides constant at 0.53 torr is shown Fig.8. The samples grown with input ratio of 2:1 and 3:1 showed conventional microstructures with the 3:1 surface morphology being slightly less "plate-like". The 4:1 samples showed different morphologies with the outside of the tow showing regions of cluster formation wherein the growth seemed to be occurring independently of the substrate, and the inside of the

tow showing fine-grained microstructure. Although all the coatings were less than a micron thick and showed only mullite peaks in X-ray diffraction, the Al/Si ratio measured at the surface of these coatings showed significant differences (Fig.9). TEM studies performed on monolithic SiC [16] have indicated that samples grown with lower Al/Si ratios have thicker (Si-rich) amorphous interfacial layers. It is possible that a similar effect might be contributing to this observed difference in Al/Si ratios on the surface of these coated fibers.

3.2 Structure of Mullite Coating

A schematic of the proposed structure of a mullite coating on SiC fibers is shown in Fig.10. Mullite coatings were observed to start as nano-crystallites on the amorphous interface and then transition to much larger "platelet-like" columnar grains. The thickness of the nano-crystalline zone was found to depend on the growth rate, with slower growth rates yielding thicker zones. The transition from nano-crystalline to columnar platelets is projected to be the result of preferential growth along certain crystalline directions on correctly oriented grains.

3.3 Oxidation Testing

Nicalon fibers are known to degrade at temperatures around 1000°C due to carbo-thermal degradation [19]. Although the reactions involved are not fully resolved, one set of reactions proposed [20] are that silicon-oxycarbide (Si_3C_4O) pyrolyses to form SiO gas;

$$Si_3C_4O \rightarrow SiO_{(g)} + 2C + 2SiC$$

which reacts with free carbon to from CO gas;

$$SiO + 2C \rightarrow CO_{(g)} + SiC$$

so consequently the Nicalon fiber pyrolyzes to form SiC and CO;

$$Si_3C_4O \rightarrow CO_{(g)} + 3SiC$$

This results in significant weight loss due to volatilization. However, in the presence of oxygen SiC reacts to form SiO_2 which contributes to weight gain;

$$SiC_{(s)} + 1.5\ O_2 \rightarrow SiO_{2(s)} + CO_{(g)}$$

Therefore during oxidation both mechanisms are at work and consequently the weight measured is the resultant of the two competing mechanisms. However, the dominant mechanism is that of silica formation [21].

All uncoated fibers developed silica scale (cristobalite) as confirmed by the significant weight gain observed during testing. Additionally, other surface defects such as pitting (due to volatilization of the fiber) and bubbled surfaces (due to CO and SiO entrapment in the silica layer) were also observed (Fig.11). On the other hand, mullite coatings yielded excellent protection to Nicalon fibers. SEM analysis of the coated fibers indicated no surface damage. Extensive cross-sectional examination showed undamaged interfaces, and no structural changes. Nonetheless, significant damage at the uncoated ends was observed in all cases (Fig.12).

Testing at 1000°C indicated that even though mullite coated samples provided protection, the uncoated samples themselves did not degrade significantly (Fig.13).

However, when the samples were tested at 1300°C the superior performance of mullite coated Nicalon (Fig.14) and Hi-Nicalon (Fig.15) tows was evident.

3.4 Cyclic Oxidation

The inclusion of coated fibers in composites that are targeted for applications which are routinely subjected to thermal cycling, introduce further constraints such as i) thermal shock resistance of the protective coating, and ii) low thermal expansion mismatch between the coating and the fiber, to avoid spallation. Mullite coated fibers showed no spallation and negligible weight gain after 250 cycles at 1000°C (Fig.16). X-ray diffraction (Fig.17) indicated no structural changes in the coating. However, as has been reported [22], grain growth in the fibers was observed as confirmed by the sharpening of the β SiC (111) peak at 35°.

3.5 Hot Corrosion

Alkali impurities (such as Na) in fuel systems are a major concern due to hot corrosion degradation of SiC fibers [23]. The formation of a silica scale on the surface of SiC fibers has been discussed earlier. In the presence of Na_2SO_4 the following additional reactions are expected to occur:

$$xSiO_{2(s)} + Na_2SO_{4(l)} \rightarrow Na_2O.\ xSiO_{2(l)} + SO_3$$

$$Na_2SO_{4(l)} \rightarrow Na_2O_{(s)} + SO_{3(g)}$$

$$Na_2O_{(s)} + xSiO_{2(s)} \rightarrow Na_2O.\ xSiO_{2(l)}$$

Thus in the presence of the Na_2SO_4 the protective silica scale is converted to a liquid which is no longer protective. Additionally, transport rates throughout the liquid are much higher contributing to increased rate of attack of the substrate.

In the case of SiC fibers the silica layer formed is simultaneously expected to react at the interface with the free carbon in the substrate [24] resulting in additional degradation as follows:

$$SiO_{2(s)} + C_{(s)} \rightarrow SiO_{(g)} + CO_{(g)}$$

Obviously this reaction is accompanied by a weight loss and the evolved gasses are expected to diffuse through the silica layer. Kim, et al. [24] have suggested that beyond a certain thickness of the silica layer the diffusion distances become too large and the gasses get trapped, reducing further degradation. However, it is projected that since the scale is expected to liquefy, it is not likely to trap any of the reaction gasses, and the degradation reaction will not be slowed down. This might partly explain the significant weight loss observed in the fibers (Fig.18).

Several distinct types of damage due to corrosion were observed in the uncoated fibers (Fig.19). In contrast the mullite coated samples showed very good protection. Figure 20 shows the cross section and surface of the coated fiber after the test. It can be seen that both the coating-fiber and coating-salt interfaces are clean. However, uncoated ends showed extensive damage. To a very limited degree (<5%) some silica formation on the surface of the coated fiber was observed. It is not clear if this was due to non-uniform coating or occasional cracks obtained due to handling of the fibers.

3.6 Tensile Strength

Preliminary single fiber tensile test showed strength drops, due to mullite coatings, that were alarming, especially since the coatings were typically found to be crack free. Average strength values for coated Nicalon were 11.9 $\pm$ 3.7gm, coated Hi-Nicalon were 17.7 $\pm$ 5.6 gm, and both types of uncoated fibers were measured to be around 43.1$\pm$ 6.2 gm. The reason for this higher than expected degradation in strength needs to be investigated.

4.0 CONCLUSION

A modified CVD process to deposit crystalline mullite coatings on SiC fibers has been developed. Growth rate was found to have a exponential dependence on system pressure and input gas velocity. Coatings grown using partial pressure of metallic chlorides higher than 0.53 torr showed a decrease in growth rate due to depletion and gas phase nucleation. Structural investigation showed that plate-like columnar mullite grains develop out of nano-crystalline mullite zones that nucleate on amorphous interfacial layers. The thickness of the two zones was found to depend on the growth rate. Oxidation tests performed on mullite coated Nicalon and Hi-Nicalon fibers showed excellent protection up-to 200 hours at 1300°C. The coatings also performed well in a cyclic oxidation test carried out for 250 cycles at 1000°C and a sodium sulfate hot corrosion test performed at 1200°C.

5.0 ACKNOWLEDGEMENTS

Research sponsored by the U.S. Departmenmt of Energy, Assistant Secretary for Energy Efficiency and Renewable Energy, Office of Transportation Technologies, as part of the Ceramic Technology Project of the Propulsion System Materials Program, and Fossil Energy AT&TD Materials Program under contract numbers DE-AC05-960R22464 with Lockheed Martin Energy Research Corp. The authors would like to acknowledge Arun K Pattanaik, Edgar Lara Curzio, Dave Stinton, and R. Lowden for their help.

6.0 REFERENCES

1. R. W. Goettler, S. Sambasivan, and V.Dravid, *Creamic Eng. and Sci. Proc.*, 18 (3) 279 (1997).
2. N.S. Jacabson, *J. Am. Ceram. Soc.* 76 (1) (1993).
3. Parthasarthy, *J. Am. Ceram. Soc.*, 78 (7) (1995).
4. R.A. Lowden, *ORNL/TM-11039*,March,1989.
5. R.A. Lowden, *Ceramic Transactions*, 19 619-630 (1991).
6. R.A. Lowden, *Proc. of 12th Annual Conf. on Fossil Energy Materials*, 1998.
7. N.I. Baklanova, M.A. Korchagin, V.N. Kulyukin and N.Z. Lyakhov, *J.Mat. Syn. and Proc.*, 6 (1) 15- 20 (1998).
8. L.A. Akshay, D.M. Dabba and M. Sarikaya, *J. Am. Ceram. Soc.*, 74 (10) 2343 (1991).
9. P.F. Becher, *J. Am. Ceram. Soc.*, 74 (2) 255 (1991)
10. S. Somiya and Y. Hirata, *Am. Ceram. Soc. Bull*, 70 (10) 1624 (1991).
11. J. Schienle and J. Smyth, Final Report, *ORNL.Sub/84-47992/1* (1987).

12. K. Okada and N. Otsuka in S.Somiya (ed.), *American Ceramic Society, Ceramic Transactions*, 6 425 (1990).

13. O.R. Monteiro, Z.Wang and I.G. Brown, *J. Mater. Res.*, 12 (9) 2401 (1997).

14. K.N. Lee, R.A. Miller and N.S. Jacabson, *Advances in Ceramic -Matrix Composites, Ceramic Transactions*, 38 565 (1994).

15. V.K. Sarin and R.P. Mulpuri, *U.S. Patent No. 5,763,008* (1998).

16. Ping Hou, S.N.Basu and V.K.Sarin, *J.Mater.Res.*, 14 (7) 2952 (1999).

17. D. Dopalapudi, *Masters Thesis*, Boston University, 1996.

18. M.Auger, *Ph.D thesis*, Boston University, 1999.

19. M. Huger, S. Souchard and C. Gault, *J. of Mat. Sci. Letters*, 12 414-416 (1993).

20. T. Ishikawa, *Composites Sc. and Tech.*, 51 135-144 (1994).

21. N.I. Baklanova, M.A. Korchagin, V.N. Kulyukin and N.Z. Lyakhov, *J.Mat. Syn. and Proc.*, 5 (6) 425- 430 (1997).

22. C. Vahlas, P. Rocabois, C. Bernard, *J. of Matr. sci.*,.29 (22) 5839 (1994).

23. N. S. Jacabson and D.S. Fox, *J. Am. Ceram. Soc.*,79 (9) 2489 (1996).

24. Hyoun-Ee Kim and A.J. Moorhead, *J. Am. Ceram. Soc.* 74 (3) 666-669 (1991).

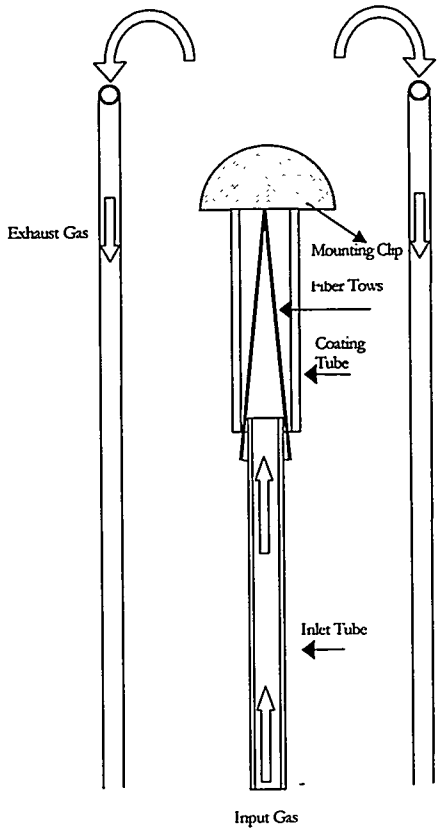

Figure 1: Schematic of fixture used to coat fiber tows.

Figure 2: SEM micrograph showing bridging in SiC fiber tows.

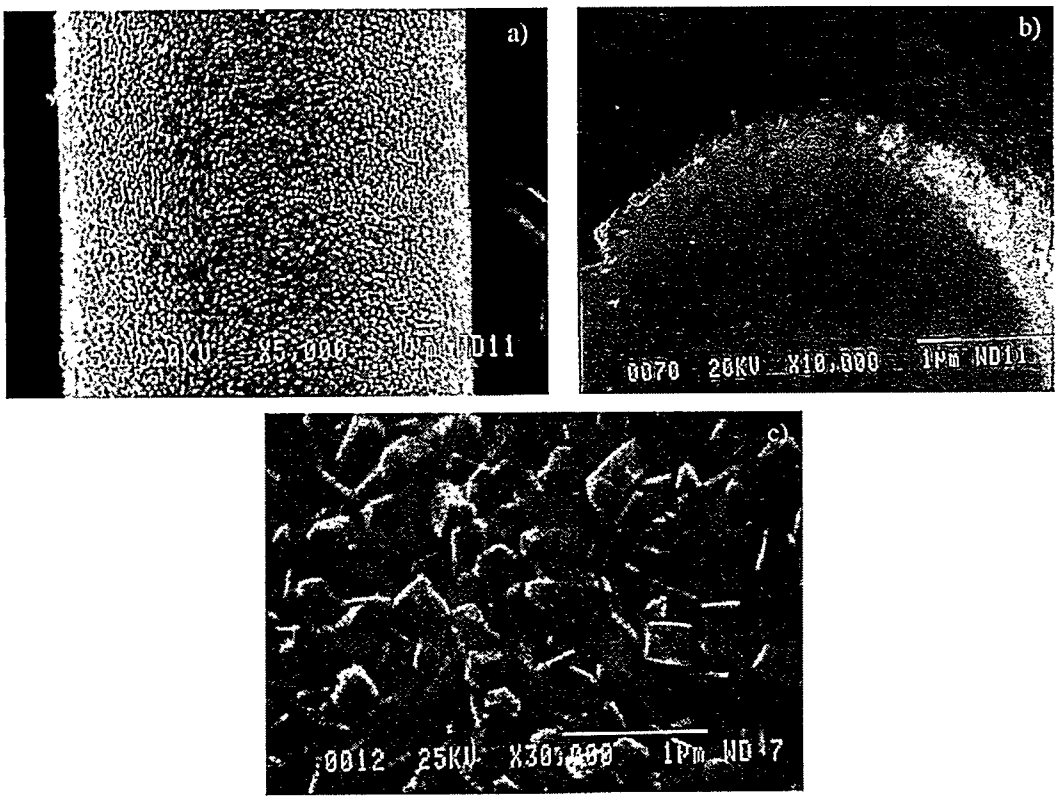

Figure 3: Micrographs showing mullite coated fiber, surface morphology and cross-section.

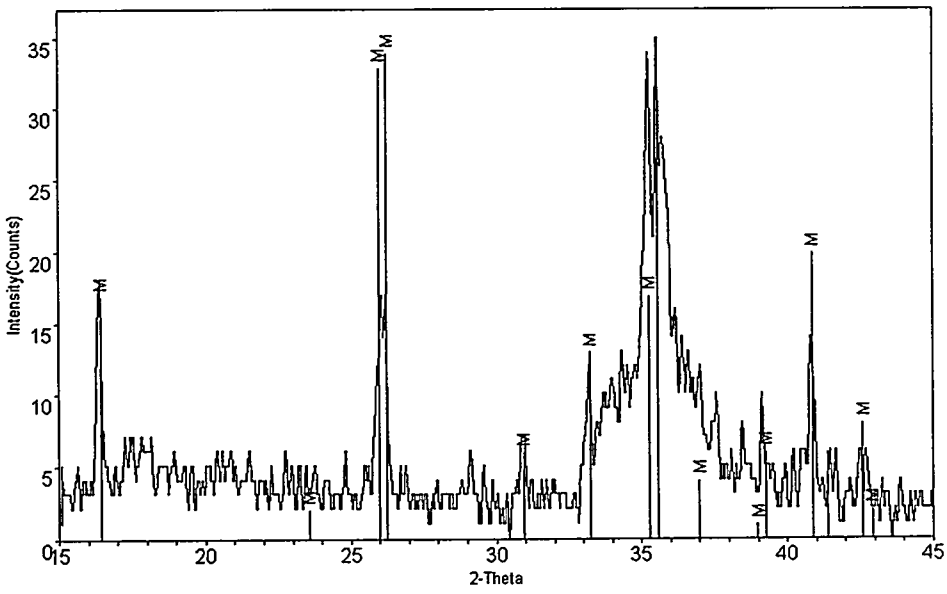

Figure 4: X-ray pattern from a mullite coated Nicalon tow.

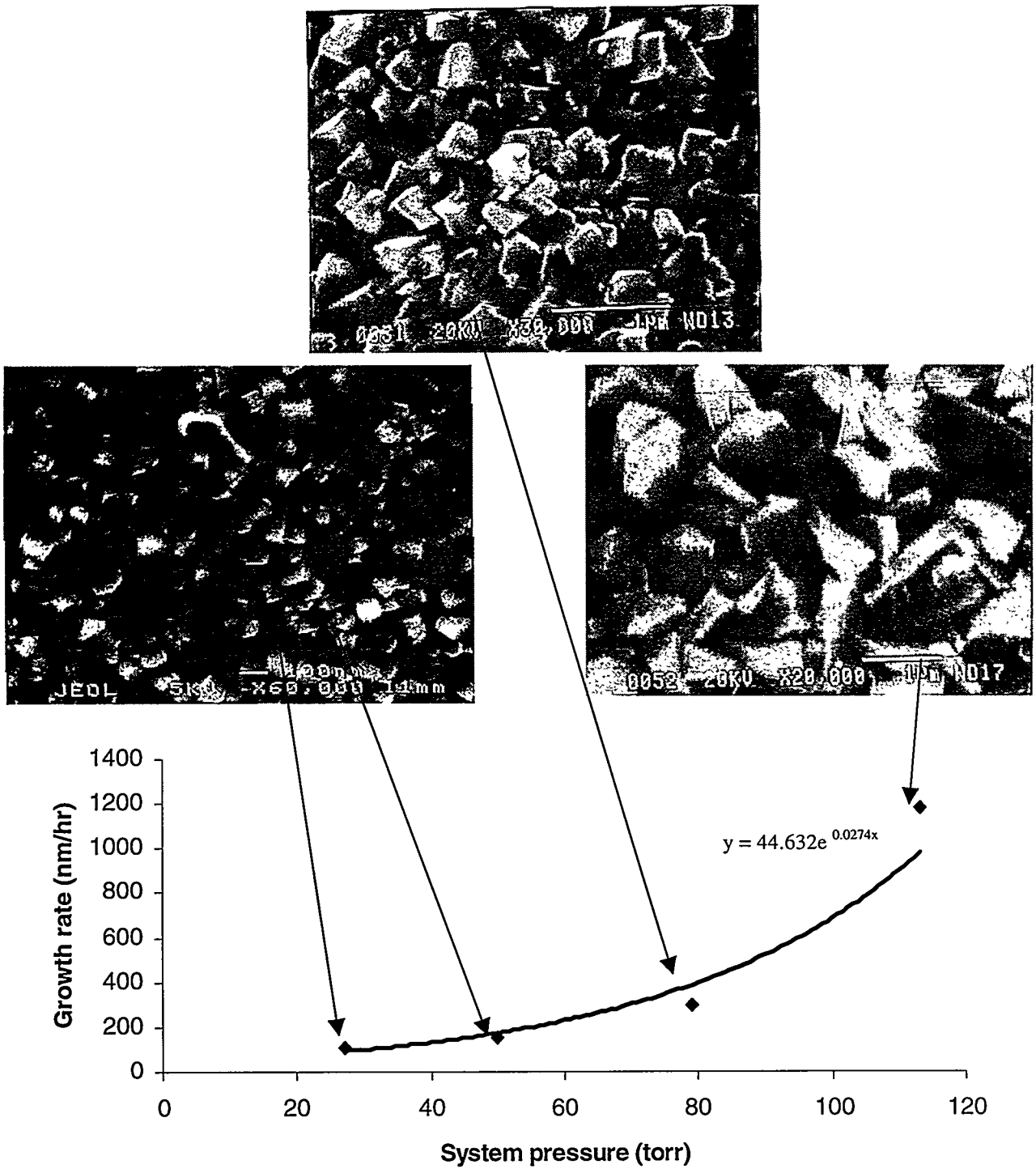

Figure 5: Effect of system pressure on growth rate and microstructure.

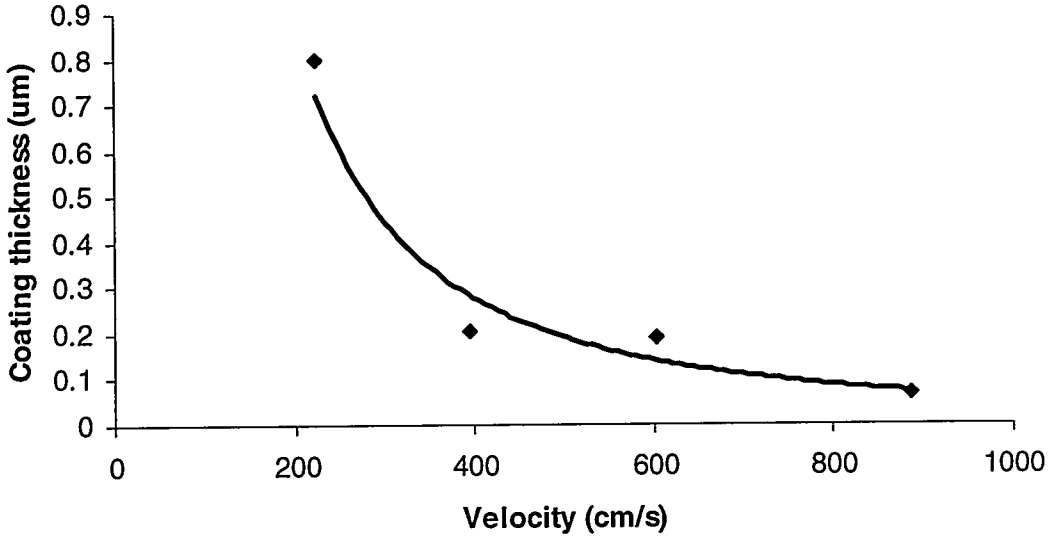

Figure 6: Coating thickness vs. input gas velocity

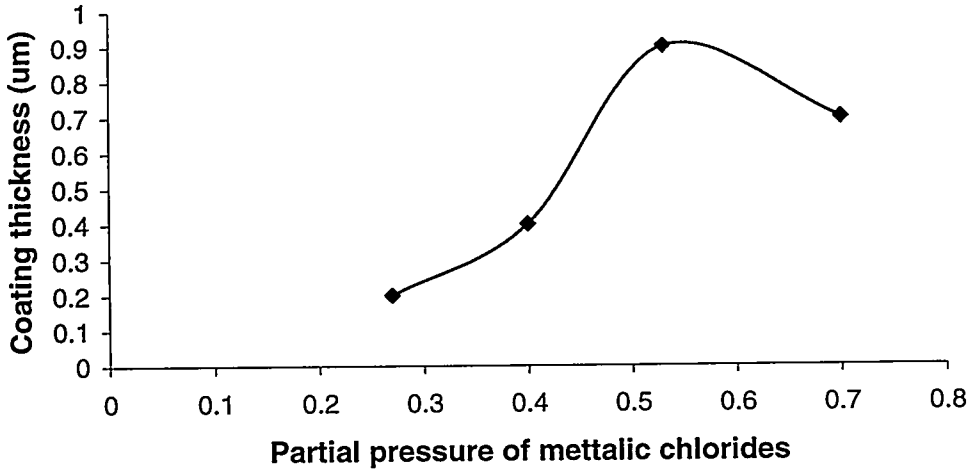

Figure 7: Coating thickness vs. partial pressure of metallic chlorides

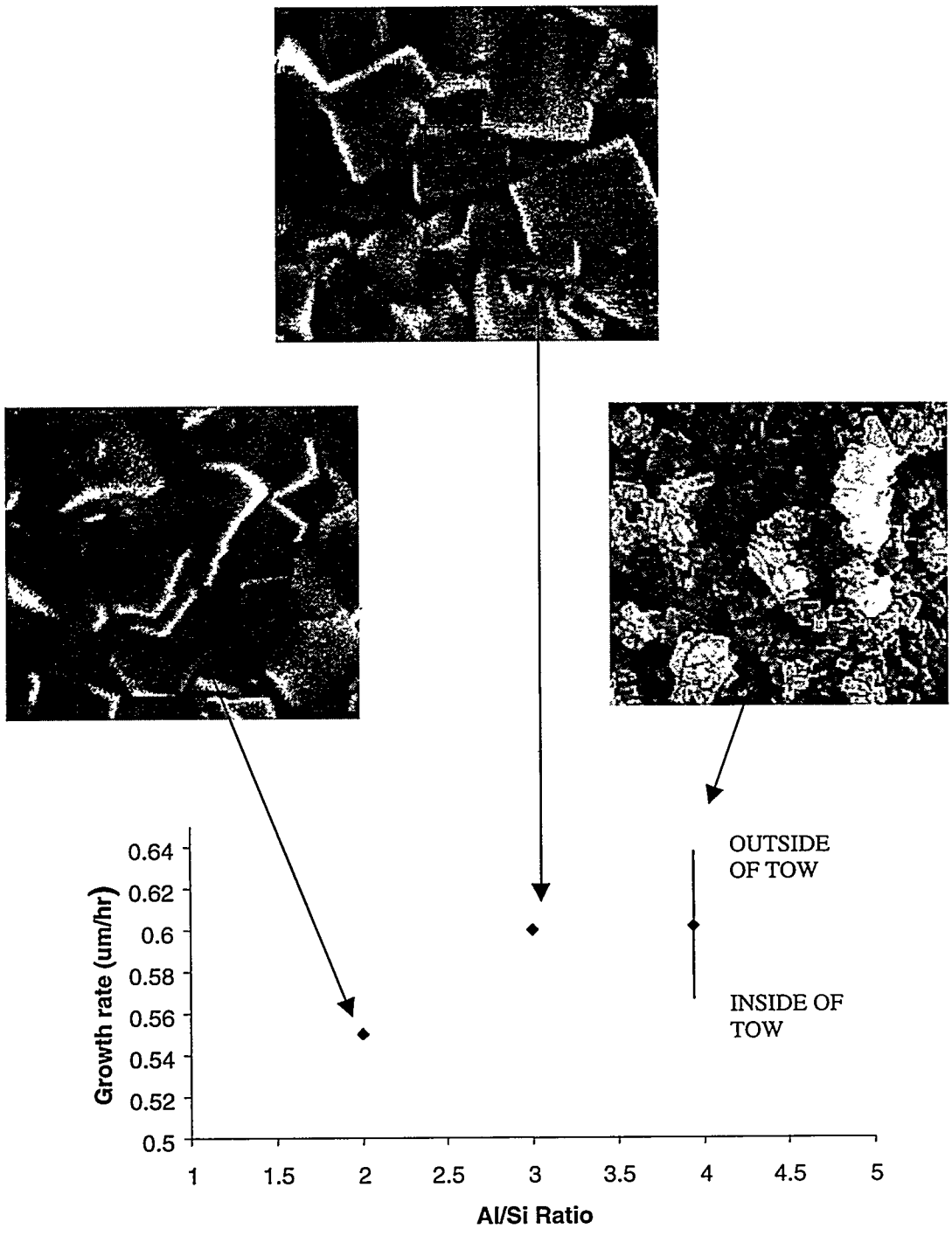

Figure 8: Effect of Al/Si ratio in the input gas at a constant partial pressure of metallic chloride.

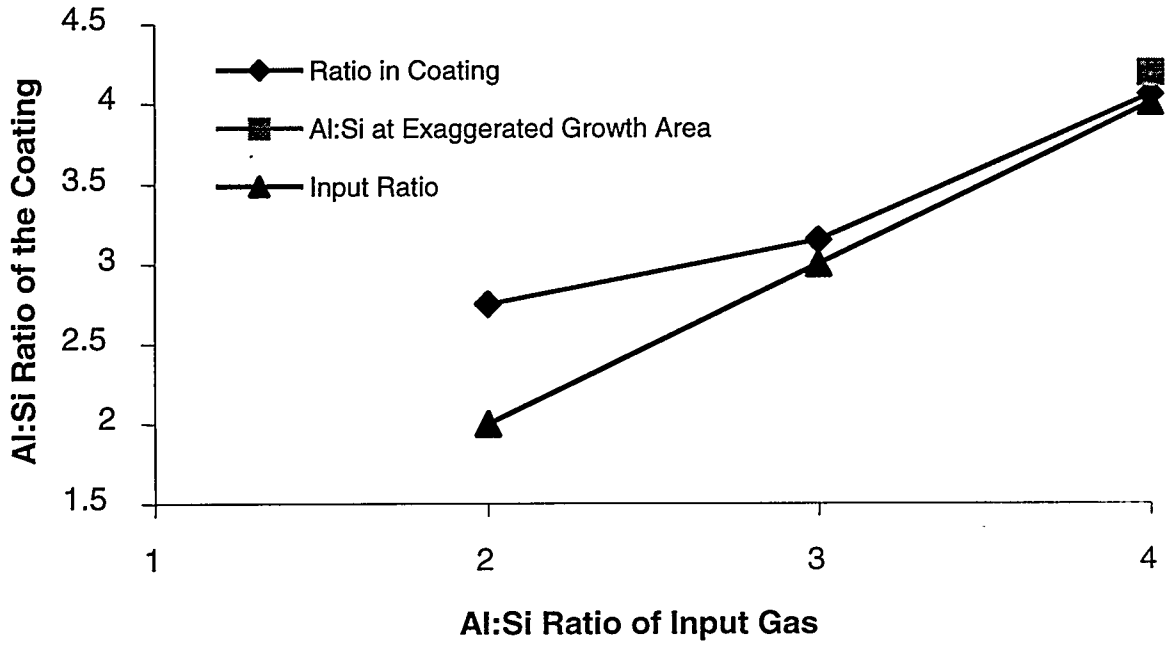

Figure 9: Plot of Al/Si ratio at the surface of the coating vs. Al/Si ratio in input gas.

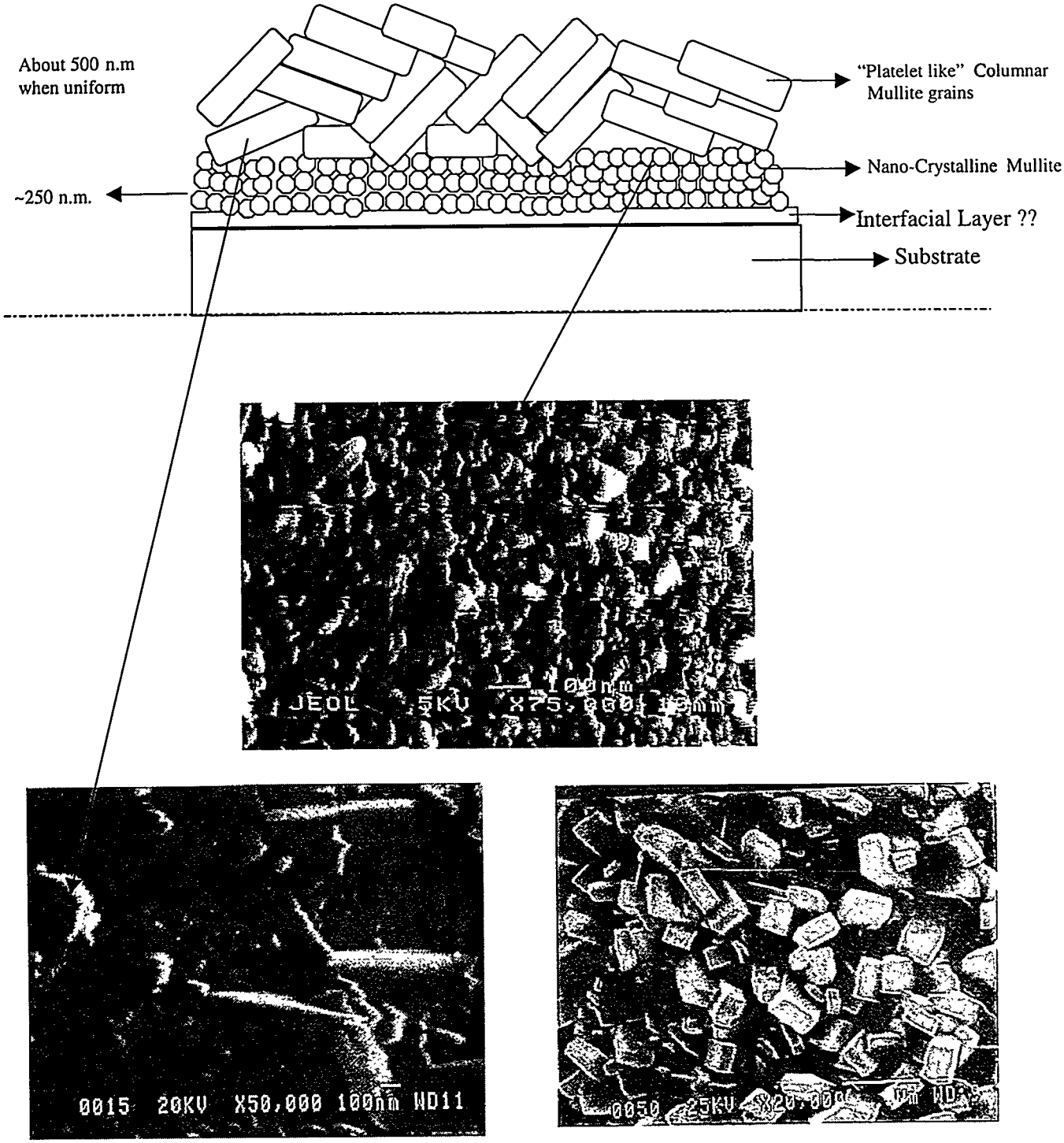

Figure 10: Structure of mullite coating on SiC fibers.

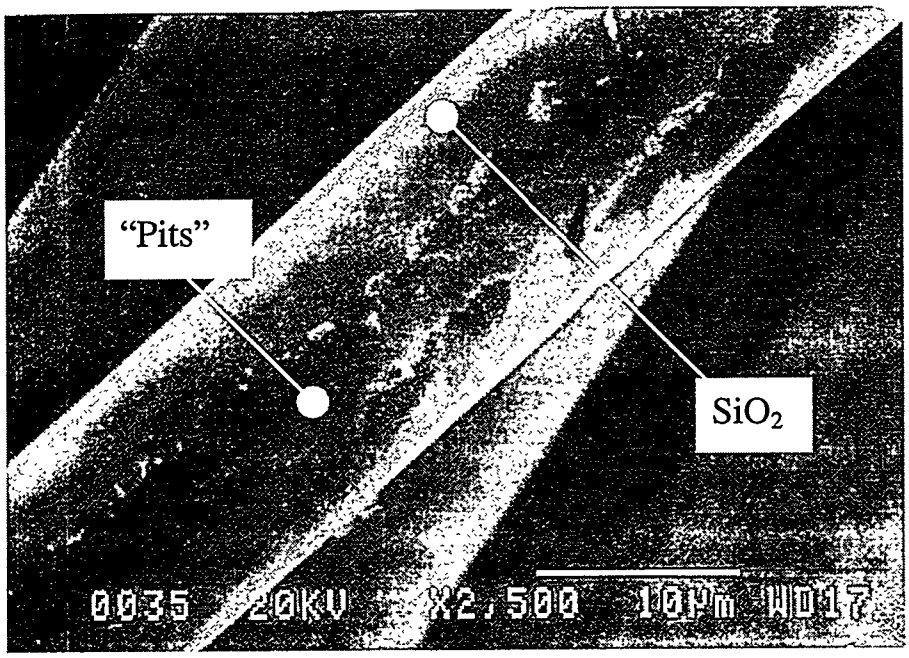

Figure 11: Surface of uncoated fibers after oxidation testing.

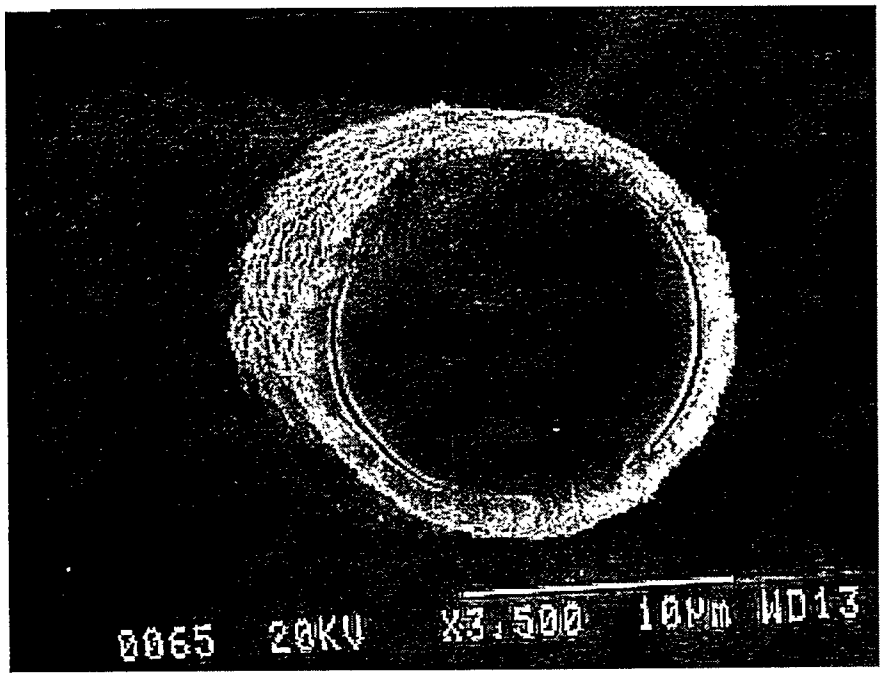

Figure 12: Uncoated end of coated fibers showed damage due to oxidation testing.

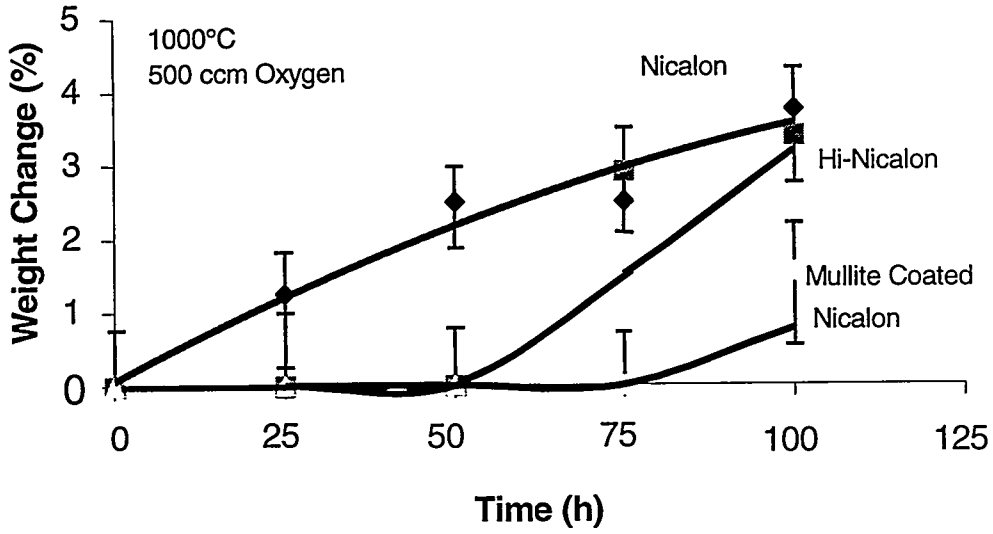

Figure 13: Performance of uncoated and coated tows during oxidation testing at 1000°C.

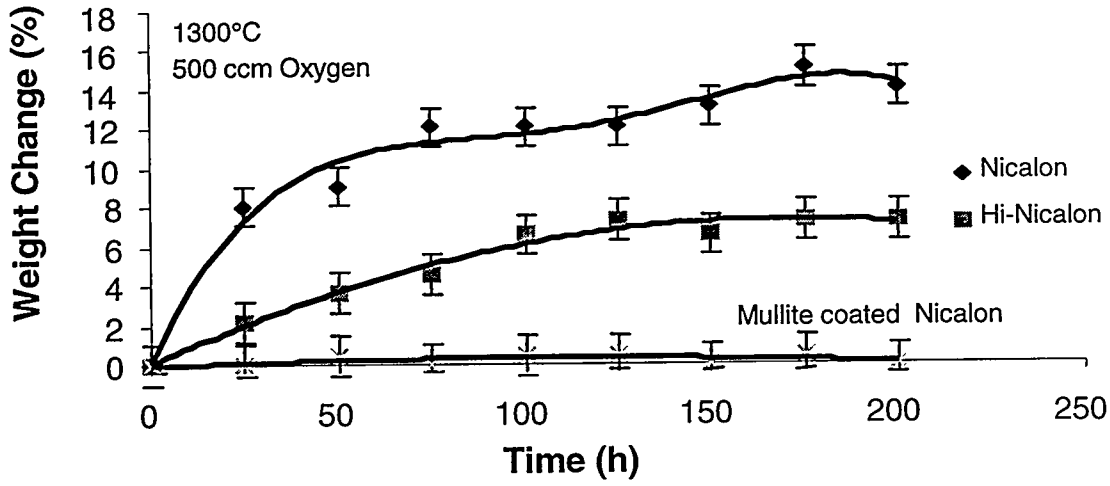

Figure 14: Weight change vs. time for uncoated and coated tows at 1300°C.

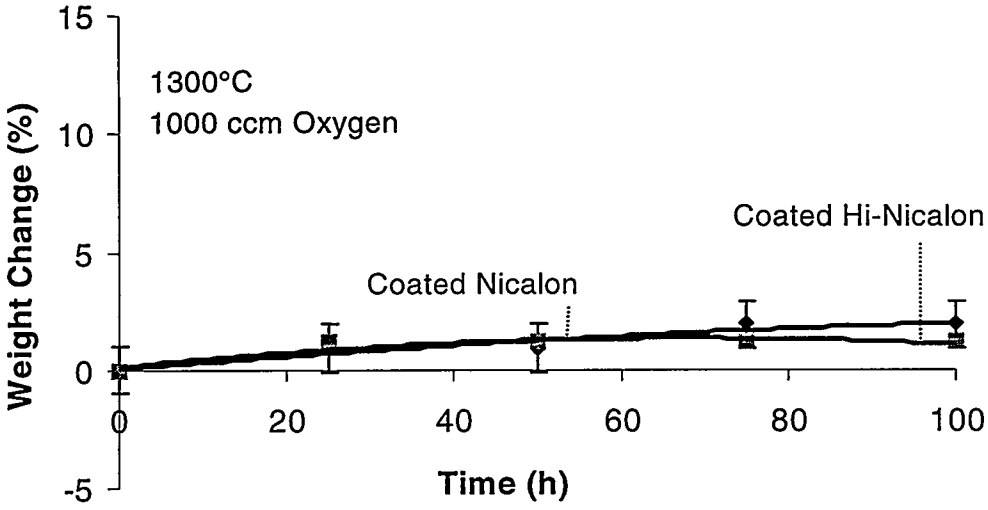

Figure 15: Comparison of performance of coated Nicalon and Hi-Nicalon.

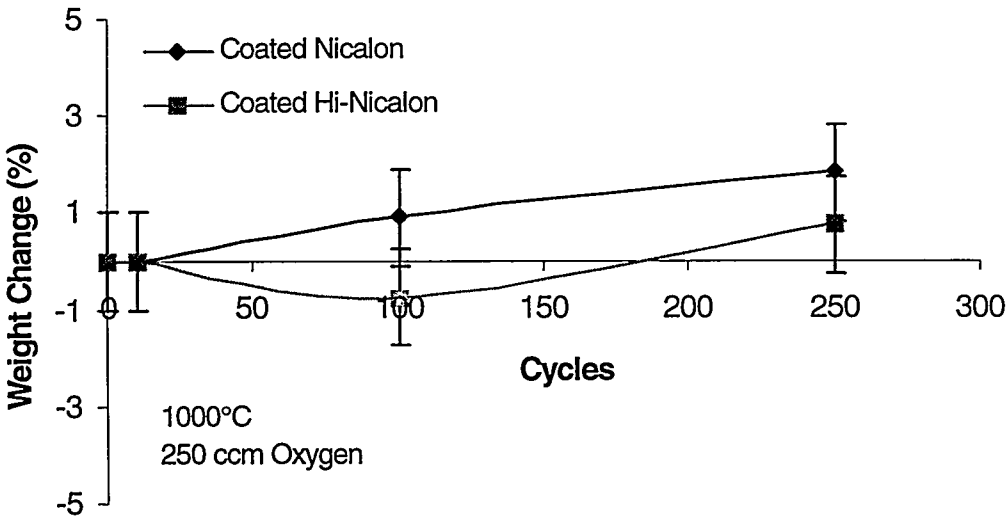

Figure 16: Weight change vs. cycles for coated Nicalon and Hi-Nicalon during cyclic oxidation testing.

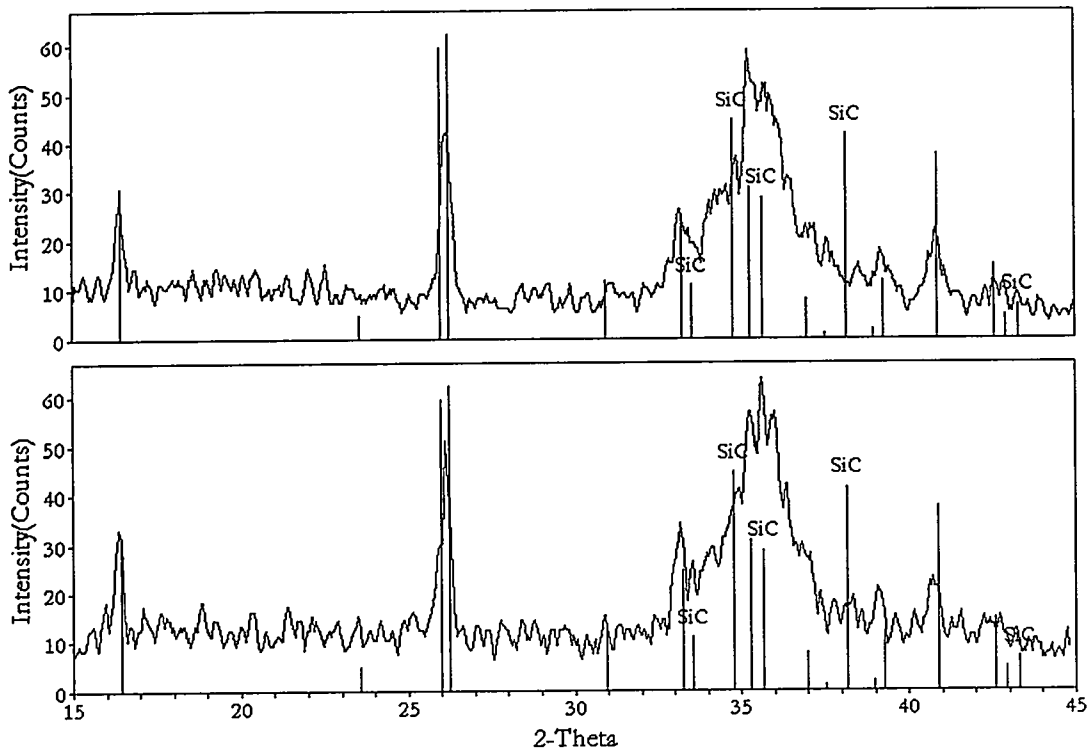

Figure 17: XRD pattern of coated Nicalon before and after cyclic oxidation testing. Un-marked peaks are from the coating.

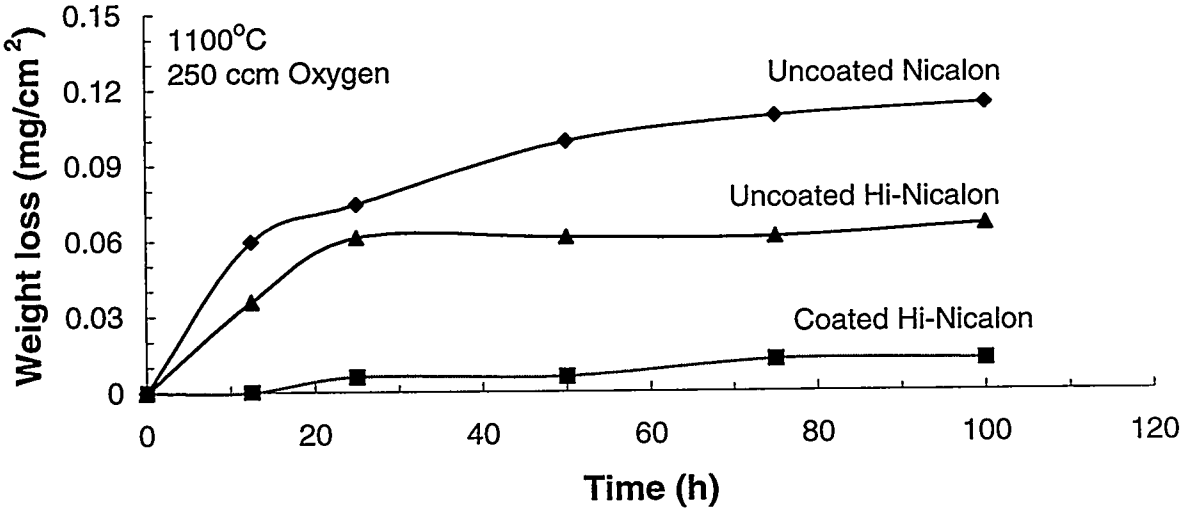

Figure 18: Weight loss vs time after hot corrosion testing.

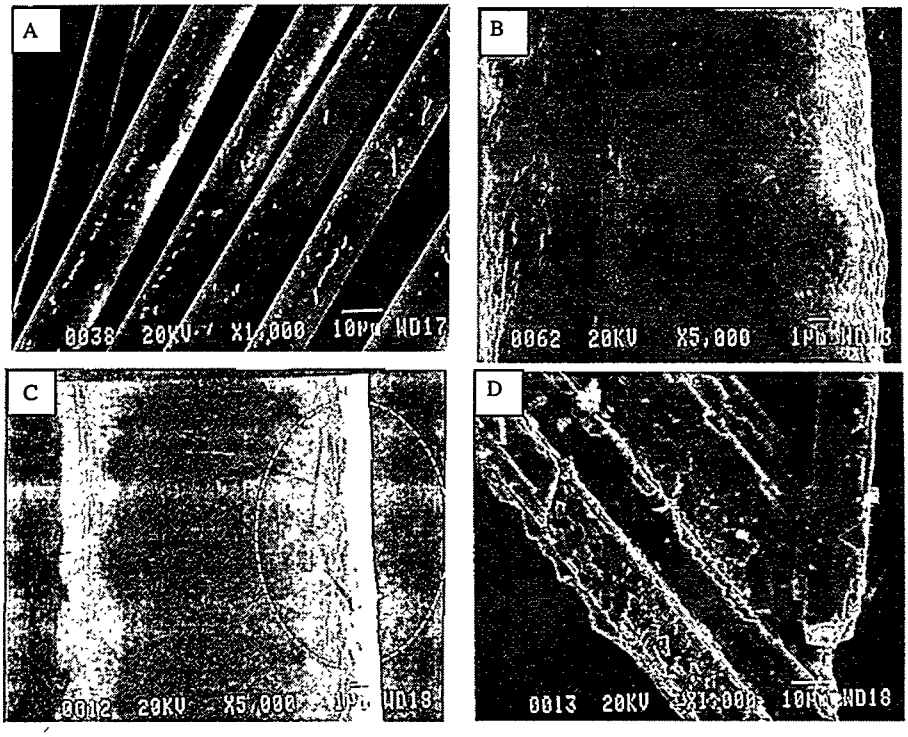

Figure 19: SEM micrographs showing A) Pitting and smooth surface , B) Bubbled surface, C) Cracked surface and D) Bridged fibers.

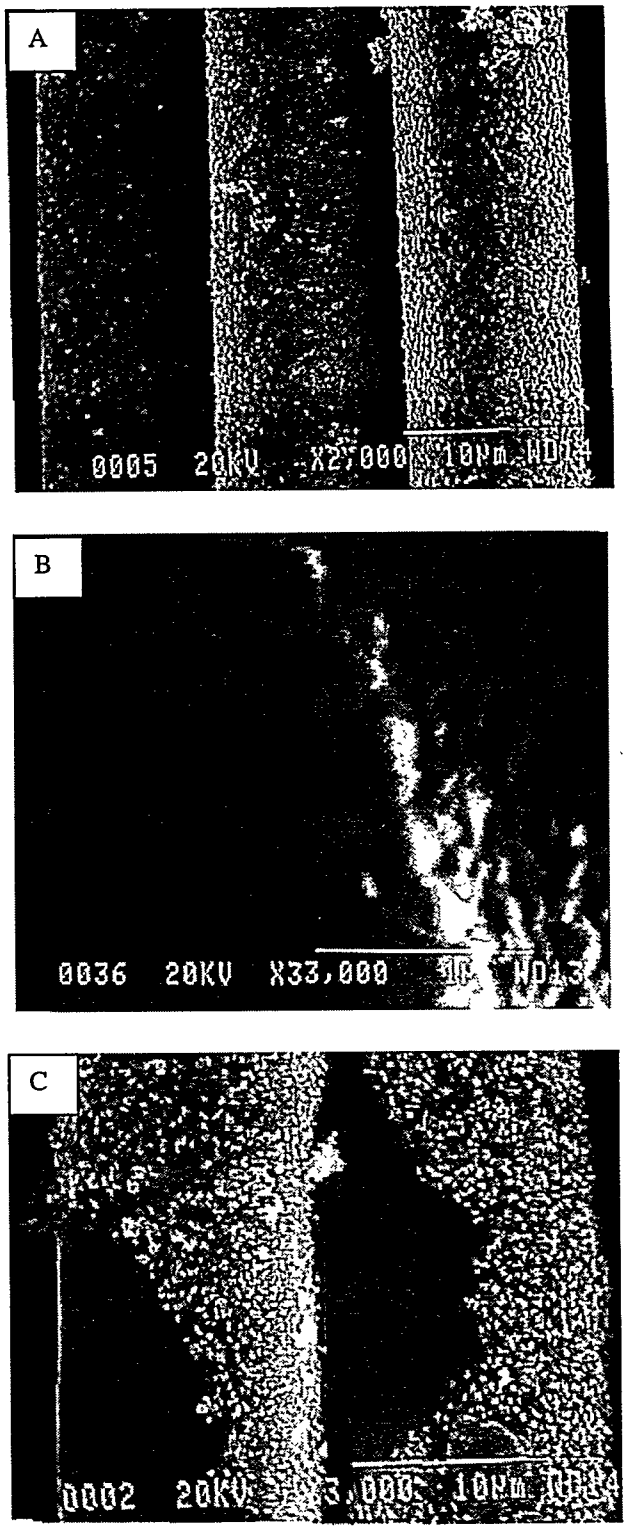

Figure 20: SEM Micrographs showing A) Undamaged coated fibers after corrosion testing B) undamaged interface and C) Few (<5%) damaged fibers.

CERAMIC COMPOSITES DISTRIBUTION

3M COMPANY
Ceramic Materials Department
201-4N-01 3M Center,
St. Paul, MN 55144
M. A. Leitheiser

AIR PRODUCTS AND CHEMICALS
P.O. Box 538
Allentown, PA 18105
S. W. Dean

ALBANY RESEARCH CENTER
1450 Queen Avenue, SW
Albany, OR 97321
R. P. Walters

ALLISON GAS TURBINE DIVISION
P.O. Box 420
Indianapolis, IN 46206-0420
P. Khandelwal (Speed Code W-5)
R. A. Wenglarz (Speed Code W-16)

AMA RESEARCH & DEVELOPMENT CENTER
5950 McIntyre Street
Golden, CO 80403
T. B. Cox

ARGONNE NATIONAL LABORATORY
9700 S. Cass Avenue
Argonne, IL 60439
W. A. Ellingson

BABCOCK & WILCOX
Domestic Fossil Operations
20 South Van Buren Avenue
Barberton, OH 44023
M. Gold

BOSTON UNIVERSITY
Manufacturing Engineering
44 Cummington Street
Boston, MA 02215
V. Sarin

BRITISH COAL CORPORATION
Coal Technology Development Division
Stoke Orchard, Cheltenham
Glocestershire, England GL52 4ZG
J. Oakey

DOE
NATIONAL ENERGY TECHNOLOGY LABORATORY
3610 Collins Ferry Road
P.O. Box 880
Morgantown, WV 26507-0880
R. C. Bedick
D. C. Cicero
R. A. Dennis
N. T. Holcombe
W. J. Huber
T. J. McMahon
J. E. Notestein

DOE
NATIONAL ENERGY TECHNOLOGY LABORATORY
626 Cochrans Mill Road
P.O. Box 10940
Pittsburgh, PA 15236-0940
A. L. Baldwin
G. V. McGurl
U. Rao
L. A. Ruth
T. M. Torkos

DOE
DOE OAK RIDGE OPERATIONS
P. O. Box 2008
Building 4500N, MS 6269
Oak Ridge, TN 37831
M. H. Rawlins

DOE
OFFICE OF FOSSIL ENERGY
FE-72
19901 Germantown Road
Germantown, MD 20874-1290
F. M. Glaser

DOE
OFFICE OF VEHICLE AND ENERGY R&D
CE-151 Forrestal Building
Washington, DC 20585
R. B. Schulz

ELECTRIC POWER RESEARCH INSTITUTE
P.O. Box 10412
3412 Hillview Avenue
Palo Alto, CA 94303
W. T. Bakker
J. Stringer

EUROPEAN COMMUNITIES JOINT RESEARCH CENTRE
Petten Establishment
P.O. Box 2
1755 ZG Petten
The Netherlands
M. Van de Voorde

LAWRENCE LIVERMORE NATIONAL LABORATORY
P.O. Box 808, L-325
Livermore, CA 94550
W. A. Steele

NATIONAL MATERIALS ADVISORY BOARD
National Research Council
2101 Constitution Avenue
Washington, DC 20418
K. M. Zwilsky

OAK RIDGE NATIONAL LABORATORY
P.O. Box 2008
Oak Ridge, TN 37831
T. M. Besmann
P. T. Carlson
J. M. Crigger (3 copies)
R. R. Judkins
R. A. Lowden
D. P. Stinton

OFFICE OF NAVAL RESEARCH
Code 431, 800 N. Quincy Street
Arlington, VA 22217
S. G. Fishman

REMAXCO TECHNOLOGIES, INC.
1010 Commerce Park Drive
Suite I
Oak Ridge, TN 37830
R. D. Nixdorf

SHELL DEVELOPMENT COMPANY
WTC R-1371
P.O. Box 1380
Houston, TX 77251-1380
W. C. Fort

TENNESSEE VALLEY AUTHORITY
Energy Demonstration & Technology
MR2N58A
Chattanooga, TN 37402-2801
C. M. Huang

THE JOHNS HOPKINS UNIVERSITY
Materials Science & Engineering
Maryland Hall
Baltimore, MD 21218
R. E. Green, Jr.

THE NORTON COMPANY
High Performance Ceramics Division
Goddard Road
Northborough, MA 01532-1545
N. Corbin

UNION CARBIDE CORPORATION
Linde Division
P.O. Box 44
175 East Park Drive
Tonawanda, NY 14151-0044
Harry Cheung

UNITED TECHNOLOGIES RESEARCH CENTER
MS 24, Silver Lane
East Hartford, CT 06108
K. M. Prewo

UNIVERSITY OF LOUISVILLE
Dept of Chemical Engineering
Speed Scientific School
Louisville, KY 40292
T. L. Starr

UNIVERSITY OF NORTH DAKOTA
Energy and Environmental Research Center
15 North 23rd Street
Grand Forks. ND 56202
J. P. Hurley

UNIVERSITY OF WASHINGTON
Department of Materials Science and
Engineering
101 Wilson, FB-10
Seattle, WA 98195
T. G. Stoebe

VIRGINIA POLYTECHNIC INSTITUTE & STATE
UNIVERSITY
Department of Materials Engineering
Blackburg, VA 24601
K. L. Reifsnider

WESTERN RESEARCH INSTITUTE
365 N. 9th Street
P.O. Box 3395
University Station
Laramie, WY 82071
V. K. Sethi

WESTINGHOUSE ELECTRIC CORPORATION
Research and Development Center
1310 Beulah Road
Pittsburgh, PA 15235-5098
S. C. Singhal